Journal of Materials Chemistry B

Accepted Manuscript

ROYAL SOCIETY OF CHEMISTRY

www.rsc.org/materialsB

Autophagy in resin monomer-initiated toxicity of dental mesenchymal cells: a novel therapeutic target by N-acetyl cysteine

*Lingxin Zhu [a], Jie Zhang [a], Lan Xiao [a], Shan Liu [a], Jingjing Yu [a], Weihai Chen [b], Xianzheng Zhang [b], Bin Peng [a,]**

[a] State Key Laboratory Breeding Base of Basic Science of Stomatology (Hubei-MOST) & Key Laboratory of Oral Biomedicine Ministry of Education, School & Hospital of Stomatology, Wuhan University, Wuhan, China.

[b] Key Laboratory of Biomedical Polymers of Ministry of Education & Department of Chemistry, Wuhan University, Wuhan, China.

* Corresponding author. State Key Laboratory Breeding Base of Basic Science of Stomatology (Hubei-MOST) & Key Laboratory of Oral Biomedicine Ministry of Education, School & Hospital of Stomatology, Wuhan University, 237 Luoyu Road, Wuhan 430079, P.R. China. Tel: + 86 27 87161981; fax: +86 27 87873260.

E-mail address: phs301@vip.163.com (B. Peng)

Acknowledgements

The authors deny any conflicts of interest related to this study. The authors are grateful for the support by grants from the National Natural Science Foundation of China (no. 81371131, 81300872, and 81170956), Specialized Research Fund for the Doctoral Program of Higher Education of China (no. 20120141110021 and 20130141120087), Hubei Province's Outstanding Medical Academic Leader Program, and Natural Science Foundation of Hubei Province of China (no. 2014CFA059).

ABSTRACT

Dental restorative biomaterials are commonly used to restore the teeth impaired by caries, erosion, or fracture. Resin monomers released from polymerized restorative composite materials could disturb cell viability and cause toxicity of oral eukaryotic cells, which remains a medical challenge. However, the intracellular processes or underlying mechanisms of resin monomer-mediated toxicity and potential preventive/therapeutic strategy are still far from clear. The present study aimed to determine the role of autophagy in resin monomer triethylene glycol dimethacrylate (TEGDMA)-induced cytotoxicity and explore autophagy as the potential therapeutic target by anti-oxidant N-acetyl cysteine (NAC) *in vitro* and *ex vivo*. Results showed that TEGDMA exposure resulted in several specific features of autophagy in human dental mesenchymal cells (DMCs), including the formation of acidic vesicular organelles, appearance of autophagic vacuoles, and LC3-II accumulation. By pharmacological and genetic approaches, the inhibition of autophagy significantly prevented TEGDMA-induced apoptosis `in DMCs. Moreover, the autophagy activated by TEGDMA occurred *via* AMPK/mTOR pathway, which could be abrogated by NAC pretreatment. More importantly, the tooth slice organ culture model provided further evidence of autophagy involvement in TEGDMA-triggered dental mesenchymal tissue toxicity and as the therapeutic target by NAC *ex vivo*. Our findings provide novel insights into the mechanisms of resin monomer-mediated toxicity and highlight autophagy as the promising therapeutic target by NAC for improving dental restorative biomaterials that enables dental tissue protection.

Key Words

Resin monomer; autophagy; N-acetyl cysteine ; dental mesenchymal cells; tooth slice organ

1 Introduction

Dental restorative biomaterials are commonly used in dentistry to aesthetically restore the structure and function of teeth impaired by caries, erosion, or fracture. The tissues of the oral cavity are harmfully affected by various biological stressors including the compounds released from dental restorative biomaterials, which may cause restoration failure and additional high costs.[1,2] Due to insufficient monomer-polymer conversion, the monomers of restorative composite resins or dentin bonding agents permeate into their surrounding aqueous environment and affect the vitality and biological activities of the adjacent living oral tissues.[1,2] Triethylene glycol dimethacrylate (TEGDMA), an ester of α, β-methacrylic acid and ethylene glycol, is a major resin co-monomer released from modern dental composites in an aqueous environment. TEGDMA has dual hydrophilic and lipophilic propertities. Hence, it may easily enter numerous biological environments, particularly the dental mesenchymal tissues.[3,4] Moreover, this resin monomer could induce various stress responses in eukaryotic cells, such as cytotoxicity, apoptosis, genotoxicity, inhibition of the mineralization process, and disturbance of the innate immune functions.[5-9]

Exploring the novel mechanism of action by resin monomers is highly attractive, because such mechanism is can provide valuable insights into therapeutic strategies for improving dental restorative biomaterials for protecting oral tissues. Considerable evidence has specified that oxidative stress with elevated reactive oxygen species (ROS) generation initiated by resin monomers modulates tightly regulated signaling pathways which control cell survival and death.[10-12] Previous studies have shown that TEGDMA significantly induces intracellular ROS generation and apoptosis.[3,4,13,14] However, the intracellular processes or signaling pathways related to ROS production and apoptosis initiated by resin monomers are yet to be clarified.

N-acetyl cysteine (NAC), an anti-oxidative amino acid derivative that could be incorporated into cells, has been identified to attenuate cytotoxicity caused by resin monomers.[4,12,15] Further understanding of intracellular therapeutic targets and pathways involved in NAC-mediated protection against resin monomer-initiated toxicity is limited and urgently needed.

Macroautophagy (hereafter referred to as autophagy) is an evolutionarily conserved and highly regulated ubiquitous cellular process that degrades intracellular components in response to stressful conditions, and is associated with various cellular processes including cell survival, cell death, pathogen clearance, and antigen presentation. In the process of autophagy, the characteristics of double- or multi-membrane autophagosomes initially form by surrounding the parts of the cytoplasm and intracellular organelles. The outer membrane of autophagosomes then fuses with lysosome or endosome, thereby generating a single-membrane autolysosome. Finally, the contents of the autolysosomes are subsequently digested by lysosome enzyme.[16,17] Among the identified autophagy-related genes (Atg), Beclin1, Atg5, Atg12, and microtuble-associated protein 1 light chain 3 (LC3, a mammalian homolog of yeast Atg8) are essential for autophagy induction.[17,18] It should be noted that autophagy could also occur in a Beclin1-independent pathway.[17,18] Autophagy could serve as either a cell survival mechanism or a cell death mechanism under different environmental stressful conditions and with various cell types. Such a process could provide energy in case of energy shortage because of bulk degradation. However, this process may also be pro-apoptotic because it could incur the self-destruction of mammalian cells.[19,20] However, to date, it remains unknown whether resin monomer could induce autophagy, and how autophagy regulates resin monomer-mediated toxicity of dental mesenchymal cells.

In the present research, we aimed to determine the autophagy induction potential by TEGDMA as a

model resin monomer, and the role of autophagy during TEGDMA-initiated toxicity, as well as to explore autophagy as potential therapeutic target by NAC in human dental mesenchymal cells (DMCs) *in vitro* and tooth slice organ culture model *ex vivo*. The possible involvements of adenosine monophosphate-activated protein kinase (AMPK)/mammalian target of rapamycin (mTOR) signaling in TEGDMA-mediated autophagy were also investigated.

2 Materials and Methods

2.1 Chemicals and reagents

TEGDMA, 3-Methyladenine (3-MA), NAC, Compound C, control siRNA, Atg5-siRNA, and TSC2-siRNA were purchased from Sigma-Aldrich (Sigma, St. Louis, USA). Fetal bovine serum (FBS), penicillin/streptomycin, phosphate-buffered saline (PBS), 2'7'-dichlorodihydrofluorescein diacetate (DCF-DA), and 5,5',6,6'-tetrachloro-1,1',3,3' -tetraethyl benzimidazole carbocyanine iodidee (JC-1) were acquired from Invitrogen Life Technology (Invitrogen, Carlsbad, USA). The antibodies specific to LC3B, Atg5, and Beclin1 were obtained from Sigma. The antibodies specific to cleaved poly(ADP-ribose) polymerase (PARP), phospho-S6, S6, phospho-AMPK, and AMPK were obtained from Cell Signaling Technology (Cell Signaling, Beverly, USA). The antibodies specific to p-mTOR and mTOR were purchased from Epitomics (Burlingame, USA) and those specific to Bcl-2, Bax, and β-actin were obtained from Santa Cruz Biotechnology (Santa Cruz, CA, USA). Hoechst 33258 and acridine orange were procured from Beyotime Biotechnology (Beyotime, Jiangsu, China). The cell counting kit-8 (CCK-8) was obtained from Dojindo (Kumamoto, Japan), whereas the Annexin V-FITC Apoptosis detection kit was purchased from BD Pharmingen (Franklin Lakes, USA). The *in situ* apoptosis detection kit by terminal deoxynucleotidyltransferase-mediated dUTP-biotin nick end labeling method (TUNEL) was purchased from Roche Diagnostics (Basel, Switzerland).

2.2 Physicochemical characterization of resin monomer TEGDMA

The physicochemical features and structure of the resin monomer TEGDMA were determined and confirmed by ultraviolet-visible (UV-VIS) spectrophotometer (Lambda Bio40, PerkineElmer), attenuated total reflectance Fourier transform infrared (ATR-FTIR; Thermo Electron Scientific

Instruments Corp., Madison, USA) spectroscopy, micro-Raman spectroscopy (LabRAM, Horiba Jobin Yvon, France), and ^{1}H NMR spectrum (Varian Mercury VX-300; Varian Inc., Palo Alto, USA).

2.3 DMCs isolation and culture

The isolation of human DMCs was performed according to the previously described methods[22], with minor modification. Experimental protocols were approved by the Ethics Committee of School of Stomatology, Wuhan University, China. Healthy human dental pulp mesenchymal tissues were obtained from extracted third molars (15-20 years of age), with informed consents obtained before tooth extraction. The dental pulp mesenchymal tissues were gently separated, minced, and digested with 3 mg/ml Collagenase type I (Invitrogen Life Technology, Carlsbad, USA) and 4 mg/ml Dispase (Gibco, Grand Island, USA) for 1 h at 37 °C. Single-cell suspensions were obtained from the digested mixtures through a 70 μm cell strainer, and seeded into 6-well plates in α-MEM supplemented with 20% FBS and antibiotics. Cell cultures were maintained at 37 °C in a humidified atmosphere with 5% of CO_2 and 95% air. After confluence, the cells were detached with 0.25% trypsin and 0.2% EDTA and were then sub-cultured at a ratio of 1:3. The DMCs between the 3th and 5th passages were used in this study.

2.4 Cell viability assay

The cell viability of DMCs was assessed with a CCK-8 kit. The DMCs were incubated with various concentrations of TEGDMA (0 mM to 10 mM) for 24, 48, and 72 h after cell seeding. Approximately 10 μL of CCK-8 solution with 90 μL α-MEM was added to each well, and the mixture was incubated for another 3 h. The optical density was measured by conducting a microplate autoreader

enzyme-linked immunosorbent assay (Bio-Tek Instruments Inc., Winooski, USA) at 450 nm.

2.5 Western blot assay

The appropriately treated DMCs were lysed in M-PER (Pierce Chemical Company, Rockford, IL, USA) buffer supplemented with proteinase inhibitor (Roche) on ice for 15 min. Protein extracts were quantified with BCA protein assay kit (Pierce), and Western blot analysis was performed according to our previous protocol.[23] Corresponding primary antibodies including cleaved PARP, phospho-S6, S6, phospho-AMPK, AMPK, p-mTOR, mTOR, Bcl-2, Bax, and β-actin were used in this study.

2.6 Detection of acidic vesicular organelles (AVOs)

The appropriately treated DMCs were stained with 1 μg/ml acridine orange in PBS for 15 min, washed with PBS, and then examined under a Leica fluorescence microscope.

2.7 Cellular immunofluorescent staining

Appropriately treated DMCs were fixed with 4 % paraformaldehyde, and immunofluorescence staining was performed with LC3 primary antibodies followed by tetramethyl rhodamine isothiocyanate-conjugated secondary antibody (Jackson ImmunoResearch Laboratories, West Grove, USA). Double immunofluorescence labeling was employed to colocalize LC3 with fibrous actin (F-actin) using FITC-conjugated phalloidin (Sigma). Nuclei were stained with 4',6-diamidino-2-phenylindole (DAPI), and coverslips were mounted on a microscope slide with the embedding medium. The cells were consequently observed and photographed with a fluorescence microscope (Leica, Germany).

2.8 Transmission electron microscopy (TEM) analysis

The appropriately treated DMCs or dental mesenchymal tissues of tooth slice organs were harvested and placed in 2.5% glutaraldehyde overnight at 4 °C. The cells or tissues were postfixed in 1% osmium tetroxide with 0.1% potassium ferricyanide. Subsequently, the cells were dehydrated through a graded series of ethanol (30% to 90%) and were embedded in Spurr's epoxy resin. Ultrathin sections were cut, stained with 2% uranyl acetate, and were examined with a Hitachi H-600 Transmission Electron Microscope.

2.9 Measurement of mitochondrial membrane potential (ΔΨm)

The lipophilic cationic dye JC-1 was used to measure the mitochondrial membrane potential $\Delta\Psi m$. This dye reagent enters the mitochondria, aggregates, and fluoresces red. When the mitochondrial membrane potential collapses, the dye reagent can no longer accumulate within the mitochondria and fluoresces green.[24] In this research, the appropriately treated DMCs were stained with 5 μg/mL JC-1 for 30 min and were analyzed with FACS Calibur flow cytometer and Cell Quest Software (Becton Dickinson, Franklin Lakes, NJ). The emission filters of 535 and 595 nm were used to quantify the population of mitochondria with green (JC-1 monomers) and red (JC-1 aggregates) fluorescence, respectively.

2.10 Measurement of intracellular ROS level

The production of intracellular oxidant was determined based on the reaction of DCF-DA and intracellular ROS, which prompted the formation of the fluorescent compound DCF.[24] Thus, for ROS

analysis, the appropriately treated DMCs were incubated with 10 μM DCF-DA for 30 min. Meanwhile, the production of DCF fluorescence representative of ROS was monitored under fluorescence microscope or by FACS Calibur flow cytometer (excitation wavelength, 488 nm; emission wavelength, 515 nm to 545 nm), and the results were analyzed with Cell Quest Software (Becton Dickinson, Franklin Lakes, NJ).

2.11 Hoechst staining for morphological evaluation

The DMCs were seeded into a 6-well plate. After the cells were incubated with 3 mM TEGDMA for the indicated durations, they were processed for Hoechst staining. In brief, the cells were fixed in 4% paraformaldehyde, washed with PBS, and stained with Hoechst 33258 dye, prior to extensive washing. Nuclear staining was examined under a fluorescence microscope (Leica).

2.12 Cell apoptosis analysis

The cell apoptosis of DMCs was assessed with Annexin V-FITC Apoptosis detection kit (BD Pharmingen, Franklin. Lakes, USA) according to the manufacturer's instructions. Briefly, the cells were collected and stained with FITC-Annexin V (green fluorescence) and propidium iodide (PI, red fluorescence) and were then incubated for 15 min in the dark. The stained cells were then examined under a FACScan Analyzer (Becton Dickinson) to determine the percentage distribution of viable (Annexin V/PI negative), early apoptotic (Annexin V positive, PI negative), late apoptotic (Annexin V/PI positive), and necrotic (Annexin V negative, PI positive) cell populations.

2.13 siRNA knockdown

DMCs were seeded into 6 cm culture dishes and were then transfected with Atg5-siRNA, TSC2-siRNA, or control siRNA using the MACSfectin™ Reagent (Miltenyi Biotec GmbH, Germany) according to the manufacturer's protocol, as previously described.[25] The cells were then subjected to autophagy or apoptosis assays, as specified above.

2.14 *Ex vivo* tooth slice organ culture model

Human tooth slice organ were obtained from extracted third molars of men and women (18 years old to 22 years old) without caries and any history of inflammation or diabetes mellitus as previously described.[26,27] This study and the consent procedures were approved by the Ethics Committee of School of Stomatology, Wuhan University, China. Coronal parts of the freshly extracted teeth were sectioned transversely into 700 μm thick sections with a diamond saw (Buehler, Whiteby, Ontario, Canada). The tooth slice organs were immediately placed in α-MEM supplemented with 10% FBS and antibiotics (100 U/mL of penicillin and 100 μg/mL of streptomycin). The tooth slice organ cultures were maintained at 37 °C in a humidified atmosphere with 5% of CO_2 and 95% air for 48 h. Then they were treated with appropriate signaling inhibitors or TEGDMA.

Some of the appropriately treated tooth slice organs were subjected to tissue viability assay and TEM analysis. The others were fixed with 4% paraformaldehyde at 4 °C for 48 h, and then rinsed and decalcified with 10% EDTA for 3 weeks, dehydrated, and embedded in paraffin. Serial sections of 4 μm thickness were cut in the horizontal direction and subjected to hematoxylin-eosin (H&E) staining, Masson's trichrome staining, and Sirius red staining as described previously,[23] as well as tissue double-labeling immunofluorescence detection.

2.15 Tissue viability assay

The viability of appropriately treated *ex vivo* tooth slice organs was assessed with a CCK-8 kit as described previously.[26] Approximately 20 μL of CCK-8 solution with 180 μL α-MEM was added to each well, and the mixture was incubated for another 3 h. The optical density was measured by conducting a microplate autoreader enzyme-linked immunosorbent assay (Bio-Tek Instruments Inc., Winooski, USA) at 450 nm.

2.16 Tissue double-labeling immunofluorescence assay

The tooth slice sections were subjected to LC3/TUNEL, LC3/p-AMPK, and LC3/p-mTOR double-labeling immunofluorescence. Briefly, after deparaffinization and rehydration, the sections were treated with 0.625% trypsin for 10 min, and non-immune goat serum for 30 min. The unwashed sections were incubated with the primary antibody of LC3 (Sigma) at 4 °C overnight. Subsequently, the sections were incubated with TRITC-conjugated secondary antibody (Jackson) for 1 h. Then for LC3/TUNEL double-labeling, the sections were incubated in permeabilization solution (10 μg/mL proteinase K) at 37 °C for 10 min and with TUNEL reaction mixture in a humid chamber at 37 °C for 60 min. For LC3/p-AMPK and LC3/p-mTOR double-labeling, the sections were incubated with the primary antibody of p-AMPK (Cell Signaling) or p-mTOR (Epitomics) at 4 °C overnight, followed by incubation with FITC-conjugated secondary antibody (Jackson) for 1 h. DAPI was counterstained to reveal the nuclei before traditional or confocal fluorescent microscopy analysis (Leica).

2.17 Statistical Analysis

All values were expressed as mean values ± standard deviation (SD). All statistical analyses were

performed using one-way ANOVA followed by Student-Newman-Keul's tests. The values were compared by using multiple comparisons, and *P* values of 0.05 or less were considered significant.

3 Results

3.1 Physicochemical characterization of resin monomer TEGDMA and its autophagy induction potential in DMCs

Several characterization methods such as UV-VIS, ATR-FTIR, micro-Raman, and ^{1}H NMR were used to investigate the physicochemical features and structure of resin monomer TEGDMA. Results showed that the UV-VIS spectra of TEGDMA possessed no absorption peak ranging from 300 to 700 nm (Fig. 1A). In the ATR-FTIR spectrum of TEGDMA, typical absorption peaks were observed at 2956 cm^{-1} (C-H), 1720 cm^{-1} (C=O), 1635 cm-1 (C=C), 1250 cm^{-1} (C-O-C), and 1152 cm^{-1} (C=O) (Fig. 1B). The micro-Raman spectra showed characteristic bands of methacrylate CCO (605 cm^{-1}), CH_2 (1453 cm^{-1}), C=C double bond reactive peaks (1410 and 1640 cm^{-1}), and carbonyl (1720 cm^{-1}) (Fig. 1C). The ^{1}H NMR spectrum further confirmed the assigned structures of TEGDMA (Fig. 1D).

CCK-8 assay was first performed to test the cell viability of DMCs exposed to different concentrations of TEGDMA under varying time conditions. The results showed that TEGDMA inhibited the cell viability of DMCs in a time- and dose-dependent manner within the dose range of 1 mM to 5 mM. A pronounced reduction (up to ~60%) in cell viability was observed in DMCs treated with 3 mM TEGDMA for 48 h (Fig. 2A). Whether autophagy was activated in DMCs after exposure to the toxic concentration of TEGDMA was subsequently investigated. As shown in Fig. 2B, 3 mM TEGDMA induced the cleavage of LC3 (an increase in the LC3-II/LC3-I ratio) in DMCs and up-regulated the expression levels of Atg5-Atg12 and Beclin1, which are essential for autophagosome formation. Moreover, we examined the autophagic response of DMCs to TEGDMA by analyzing the yellow-orange AVOs formation, and immunofluorescent Beclin1/LC3-II accumulation, which are considered the hallmarks of autophagy.[28] As illustrated in Fig. 2C, the findings indicated that the

control DMCs primarily exhibited green fluorescence. However, the treatment with TEGDMA induced the formation of yellow-orange AVOs in a time-dependent manner. Moreover, the observations demonstrated that 3 mM TEGDMA exposure led to an obviously disrupted stress fiber assembly and punctate LC3 immunostaining in DMCs that rarely ocurred in control cells (Fig. 2D). Ultrastructural analysis by TEM further confirmed that TEGDMA treatment resulted in typical appearance of membranous vacuoles resembling autophagosomes (arrow heads) in a time-dependent manner (Fig. 2E). These observations strongly suggested that TEGDMA activated autophagy in DMCs.

3.2 TEGDMA induced ROS generation and apoptosis in DMCs

Remarkable loss of mitochondrial membrane potential $\Delta\Psi m$ in DMCs was observed after TEGDMA exposure (Fig. 3A). As detected by the ROS fluorescent probe DCF-DA, a significant elevation of ROS level was markedly provoked in TEGDMA-treated DMCs (Fig. 3B). With Hoechst 33258 staining, the treatment with 3 mM TEGDMA for 48 h resulted in several apoptotic morphological features, including chromatin condensation and bright blue apoptotic bodies (arrow heads) in DMCs (Fig. 3C). Meanwhile, with Annexin V and PI double staining followed by flow cytometry, the representative 2D density plots indicated the distribution of vital, early apoptotic, late apoptotic, and necrotic cells (Fig. 3D). As shown in Fig. 3E, treatment with 3 mM TEGDMA significantly induced the apoptosis of DMCs in a time-dependent manner. The expression levels of some key apoptosis-related proteins were detected to further verify the TEGDMA-induced apoptosis in DMCs. The cleavage of PARP and the ratio of Bax/Bcl-2 in DMCs were both significantly increased by TEGDMA in a time-dependent manner (Fig. 3F).

3.3 Inactivation of Atg5 prevented TEGDMA-induced autophagy in DMCs

Atg5 is an essential protein for autophagosome formation, and Atg5-deficient can significantly diminish the number of autophagic vesicles.[29] We evaluated the role of Atg5 in TEGDMA-induced autophagy in DMCs *via* pharmacological and genetic inhibition of Atg5 prior to TEGDMA treatment. As shown in Fig. 4A-B, the AVOs formation induced by TEGDMA was significantly reduced by siRNA-Atg5 transfection. The disrupted stress fibre assembly and punctate LC3 immunostaining induced by TEGDMA in DMCs was also effectively prevented by the genetic inhibition of Atg5 (Fig. 4A, C). Moreover, 3-MA, a well known autophagy inhibitor that could decrease the expression of Atg5, significantly attenuated the TEGDMA-mediated AVOs formation and punctate LC3 immunostaining (Fig. 4A-C). Consistent with these finding, the LC3-I/LC3-II conversion induced by TEGDMA in DMCs was also effectively prevented by pharmacological and genetic inhibition of Atg5 (Fig. 4D). The above findings jointly demonstrated that TEGDMA-induced autophagy in DMCs was dependent on Atg5.

3.4 TEGDMA-mediated autophagy in DMCs was not a protective mechanism but was pro-apoptotic

Autophagy is likened to the opposite faces of Janus, as it protects eukaryotic cells and helps them survive certain stress conditions. Cell death is induced when excessive autophagy occurs.[19,20] We determined the relationship between TEGDMA-induced autophagy and apoptosis by pretreatment with 3-MA or siRNA-Atg5 transfection. As shown in Fig. 5A-C, both 3-MA treatment and siRNA-Atg5 transfection significantly reversed TEGDMA-induced apoptosis in DMCs, as evidenced by Hoechst 33258 staining and flow cytometry analysis. Moreover, pretreatment with 3-MA or transfection with

siRNA-Atg5 effectively prevented TEGDMA-mediated PARP cleavage in DMCs (Fig. 5D). These results collectively indicated that TEGDMA-induced autophagy and apoptosis were interrelated in DMCs, in which TEGDMA-mediated autophagy was a pro-apoptotic mechanism, but not a protective mechanism.

3.5 TEGDMA initiated activation AMPK/mTOR signaling in DMCs

mTOR signaling pathway is a key negative regulator of autophagic process that exists in a phosphorylated form under normal conditions and suppresses autophagy.[30,31] The energy sensor AMPK activates autophagy by inhibiting mTOR activity.[32,33] To evaluate any possible signaling pathway involved in TEGDMA-induced autophagy, we tested the alteration of AMPK/mTOR signaling pathway. As illustrated by western blot assay, the treatment with TEGDMA effectively suppressed the phosphorylation of mTOR in DMCs. Meanwhile, the expression level of phospho-S6, a key downstream target of mTOR, was also reduced by TEGDMA in DMCs (Fig. 6). We also discovered that TEGDMA increased the phosphorylation of AMPK in DMCs, and this result was consistent with the suppression of phosphorylation of mTOR and S6 (Fig. 6).

3.6 AMPK/mTOR signaling was involved in TEGDMA-induced autophagy and apoptosis in DMCs

The functional significance of AMPK/mTOR signaling in the autophagic and apoptotic responses of DMCs to TEGDMA was further determined. We used siRNA-TSC2 to enhance mTOR activity, and Compound C to inhibit AMPK. As evidenced in Fig. 7A, the results of TEM specified that the appearance of autophagic vacuoles initiated by TEGDMA was diminished by siRNA-TSC2

transfection or Compound C pretreatment. Meanwhile, the results showed that pretreatment with siRNA-TSC2 transfection or Compound C significantly prevented TEGDMA-mediated AVOs formation and punctate LC3 immunostaining in DMCs (Fig. 7B-D).

Similarly, the apoptotic DMCs induced by TEGDMA were markedly reversed by pretreatment with siRNA-TSC2 transfection or Compound C (Fig. 8A-B). Pretreatment with siRNA-TSC2 transfection or Compound C effectively blocked TEGDMA-mediated LC3-I/LC3-II conversion and PARP cleavage in DMCs (Fig. 8C). Our data collectively indicated that the tight interplay between autophagy and apoptosis induced by TEGDMA occurred through AMPK/mTOR pathway.

3.7 AMPK/mTOR-dependent autophagy as the therapeutic target of NAC against TEGDMA-induced toxicity in DMCs

We further explored the potential involvement of autophagy during NAC protection against TEGDMA-initiated DMC toxicity. As illustrated in Fig. 8A-B, the apoptotic DMCs induced by TEGDMA were markedly rescued by pretreatment with NAC. The results of TEM further illustrated that the autophagic vacuoles induced by TEGDMA was diminished by NAC pretreatment (Fig. 7A). Pretreatment with NAC significantly abrogated TEGDMA-mediated AVOs formation and punctate LC3 immunostaining in DMCs (Fig. 7B-D). Meanwhile, NAC effectively blocked TEGDMA-mediated LC3-I/LC3-II conversion and PARP cleavage in DMCs (Fig. 8C). Moreover, pre-incubation with NAC counteracted TEGDMA-induced AMPK phosphorylation and mTOR activity inhibition (Fig. 6). The abovementioned results indicated that AMPK/mTOR-dependent autophagy could serve as the therapeutic target of NAC against TEGDMA-induced toxicity in DMCs.

3.8 TEGDMA activated autophagy of dental mesenchymal tissues in a human tooth slice organ culture model *ex vivo*

To further authenticate the involvement of autophagy in TEGDMA-triggered dental mesenchymal tissue toxicity *ex vivo*, a tooth slice organ culture model was established. As shown in Fig. 9A-C, TEGDMA-irritated dental mesenchymal tissues exhibited significantly decreased tissue viability and obvious destruction of extracellular matrix, accompanied by the increased autophagic LC3 and apoptotic TUNEL signal. The colocalization of LC3 with TUNEL was also revealed (Fig. 9C), suggesting the tight interplay between autophagy and apoptosis in TEGDMA-triggered dental mesenchymal tissue toxicity *ex vivo*. To further confirm the autophagy induction by TEGDMA, dental mesenchymal tissues of *ex vivo* cultured tooth slice organs were dissected and analyzed by TEM. The observations demonstrated that TEGDMA treatment resulted in typical appearance of autophagic vacuoles (arrow heads) in a time-dependent manner (Fig. 9D).

3.9 TEGDMA-triggered autophagy of *ex vivo* cultured human tooth slice organs correlated with the AMPK activation and suppression of mTOR activity

To explore the possible relationship between AMPK/mTOR pathway and TEGDMA-induced autophagy in tooth slice organ culture model *ex vivo*, we then evaluated the expression levels of p-AMPK and p-mTOR, as well as their colocalizations with autophagic LC3 signal. As shown in Fig. 10A-B, TEGDMA treatment led to significantly increased p-AMPK expression and markedly decreased p-mTOR level in the *ex vivo* cultured tooth slice organs. We also revealed that the LC3 expression was colocalized with p-AMPK-positive and mTOR-negative cells (Fig. 10A-B).

3.10 Autophagy as the therapeutic target of NAC against TEGDMA-induced dental mesenchymal tissue toxicity in *ex vivo* cultured human tooth slice organs

To further determine the functional significance of autphagy in TEGDMA-induced dental mesenchymal tissue toxicity and NAC protecion *ex vivo*, we employed the autophagy inhibitor 3-MA, AMPK inhibitor Compound C, and NAC. As illustrated in Fig. 11A-B, the decreased tissue viability and extracellular matrix destruction of *ex vivo* cultured tooth slice organs caused by TEGDMA was significantly reversed by pretreatment with 3-MA, Compound C, or NAC. Interestingly, the punctate LC3 immunostaining and TUNEL signal induced by TEGDMA was effectively prevented by pretreatment with 3-MA, Compound C, or NAC (Fig. 11C). Ultrastructural analysis by TEM further showed that appearance of autophagosomes in TEGDMA-exposed dental mesenchymal tissues *ex vivo* was diminished by the pretreatment with 3-MA, Compound C, or NAC (Fig. 11D). These results collectively indicated the involvement of autophagy in TEGDMA-triggered dental mesenchymal tissue toxicity *ex vivo*, which could serve as the therapeutic target of NAC.

4 Discussion

It has been demonstrated that the resin monomers released from modern dental composites, particularly TEGDMA, can diffuse through dentinal tubules and can arrive at dental mesenchymal tissues in the millimolar range.[1,2] In particular, these monomers could cause cytotoxicity *via* numerous mechanisms, which are associated with oxidative stress, ROS generation, and apoptosis.[3,4,14] However, the intracellular processes or signaling pathways related to ROS production and apoptosis initiated by resin monomers are yet to be thoroughly clarified. Previous studies have reported that methacrylic acid-based substances could activate autophagy.[34,35] In the present study, we comprehensively characterized the resin monomer TEGDMA by ATR-FTIR, micro-Raman, and ^{1}H NMR, which confirmed its methacrylic structure. Of note, we further discovered that TEGDMA exposure induced autophagy and prompted the activation of AMPK/mTOR signaling in DMCs, in parallel with apoptosis. The TEGDMA-activated autophagy in DMCs was pro-apoptotic because the inhibition of autophagy significantly reduced the apoptosis induced by TEGDMA. Moreover, the autophagy and apoptosis incurred by TEGDMA in DMCs occurred via AMPK/mTOR pathway. To the best of our knowledge, this study is the first to identify the autophagy induction capabilities of resin monomers in eukaryotic cells.

Autophagy, a highly-regulated process for degrading intracellular components, may represent a general cellular response to oxidative stress.[36] Such a process involves the formation of autophagosomes, which are double-membraned vesicles that sequester cytoplasm and organelles and subsequently fuse with lysosomes to form autolysosomes, thereby degrading the contents of the vacuoles.[17,18] Recent publications have illustrated that poly(methacrylic acid) microcapsules and nanomaterials [*e.g.*, quantum dots, poly(amidoamine) dendrimers, and gold nanoparticles] could induce

autophagy in different cell types.[34,35,37-39] LC3 and Beclin 1 are the critical components of autophagy.[17] In particular, LC3 is the mammalian homolog of yeast Atg8 and localizes to autophagosomal membranes after posttranslational modifications. LC3 exists in two molecular forms, namely, LC3-I (18 kD; a cytosolic form) and LC3-II (16 kD; binds to autophagosomes). The amount of LC3-II directly correlates with the number of autophagosomes.[28] Meanwhile, Beclin1 is the mammalian ortholog of the yeast Atg6/Vps30, and is involved in the regulation of autophagy.[40] In our study, treatment with the resin monomer TEGDMA resulted in several specific autophagy features in DMCs, including the appearance of autophagic vacuoles as evidenced by TEM, the formation of acidic vesicular organelles, as well as the accumulation of Beclin1 and LC3-II. Our results of TEM, SAED, and EDX analysis showed that there partially existed 3-5 nm self-assembled nanoparticles of crystalline nature derived from TEGDMA monomer (Supplementary Fig. 1A-B). Moreover, we found these TEGDMA nanoparticles could enter and accumulate in DMCs, accompanied by the presence of autophagic vacuoles (Supplementary Fig. 1C). Our findings were in agreement with others', which reported that nanoparticles including self-assembled polymeric nanoparticles, quantum dots, and gold nanoparticles have the potential to induce autophagy.[34,35,37-40]

Of note, autophagy is involved in a complex interplay with apoptosis in both physiological and pathological settings[41,42]. In particular, this process may serve as a cell survival pathway by suppressing apoptosis in some cellular settings, whereas it could lead to programmed cell death possibly via collaboration with apoptosis in other settings. Autophagy is a dichotomous phenomenon involved in cell survival or death depending on the cell type and strength of specific stimuli.[43,44] In the current research, we assessed the possible interplay between autophagy and apoptosis initiated by TEGDMA in DMCs by using the autophagy inhibitor 3-MA and Atg5-siRNA transfection. 3-MA could suppress

autophagy via the inhibition of class III PI3K, which plays a crucial role during the initiation of autophagy.[45] Atg5 is an essential protein for activating autophagy; its deficiency could significantly interrupt such process.[29] The expression of Atg5 could also be specifically knocked down by siRNA targeting Atg5. Our results suggested that the inhibition of autophagy via treatment with 3-MA or transfection with siRNA-Atg5 significantly attenuated apoptosis induced by TEGDMA in DMCs, thereby suggesting the pro-apoptotic role of autophagy by TEGDMA.

The accumulation of intracellular ROS is the main characteristic of oxidative stress. Intracellular ROS was reported to be an important signaling molecule in mediating autophagy.[46] ROS has been demonstrated to stabilize autophagosomes during nutrient deprivation, hypoxia, ischemia reperfusion injury, and stressful conditions. The physiological levels of ROS lead to growth adaption and survival. However, excessive ROS cause irreversible cellular damage, thereby provoking autophagy and/or apoptosis.[46] The depolarization of mitochondrial membranes is among the key events associated with the accumulation of intracellular ROS. Meanwhile, the disruptions of mitochondrial membranes may incur severe problems, including the decrease in ATP synthesis, increase in ROS generation, and redistribution of pro-apoptotic mitochondrial factors.[47] The critical role of intracellular ROS in the cytotoxic response induced by TEGDMA has been highlighted in recent studies.[4,14,48] Consistent with above reports,[4,14,48] our findings showed that TEGDMA exposure resulted in significantly increased ROS generation and depolarization of mitochondria in DMCs, correlated with apoptosis induction.

Several signaling pathways, particularly the AMPK/mTOR pathway, contribute to oxidative stress-induced autophagy in mammalian cells.[32,33] mTOR was established as a key negative regulator of autophagic process. mTOR exists in a phosphorylated form under normal conditions and suppresses autophagy by inactivating Atg1 and Atg13, which are indispensable for autophagosome biogenesis.[32,33]

One of the direct downstream targets of mTOR is pS6, through which mTOR activation stimulates protein synthesis. The levels of phosphorylated pS6 could be utilized as a marker for mTOR activity.[30,31] Moreover, the conserved cellular energy sensor AMPK plays an essential role in cell growth, protein synthesis, apoptosis, and autophagy. AMPK triggers autophagy through a double-pronged mechanism involving the inhibition of suppressive effect of the mTOR complex 1 pathway and the direct activation of the ULK1 protein complex.[32] However, the possible involvement of AMPK/mTOR pathway in TEGDMA-induced cytotoxicity remains unknown. In the current study, we identified that either AMPK inhibitor or siRNA-TSC2 transfection could significantly prevent TEGDMA-mediated autophagy, as revealed by AVOs formation, punctate LC3 immunostaining, LC3-I/LC3-II conversion, and appearance of autophagic vacuoles. Meanwhile, TEGDMA-induced apoptosis in DMCs was also markedly reversed by the AMPK inhibitor and siRNA-TSC2 transfection. Based on the above observations, we revealed that the interplay between autophagy and apoptosis induced by TEGDMA in DMCs occurred via AMPK/mTOR pathway.

NAC, a well-known anti-oxidative cysteine derivative, has been frequently used for the treatment of many clinical diseases such as doxorubicin-induced cardiotoxicity, acetaminophen intoxication, and heavy metal toxicity.[49] With respect to dentistry, NAC has been recently explored to rescue the cytotoxic effects of resin monomers.[4,12,15] Mechanistically, it has been demonstrated that NAC may exert protective effects against resin monomer-induced cytotoxicity possibly by intracellular ROS scavenging and GSH replenishment.[4,12,15] Our research further specified that NAC protected against TEGDMA-induced DMCs apoptosis by attenuating AMPK/mTOR-dependent autophagy. To the best of our knowledge, this is the first report demonstrating that NAC could ameliorate resin monomer-induced cytotoxicity by targeting autophagy, highlighting that autophagy inhibition may be a

novel therapeutic target towards resin monomer-initiated toxicity.

Tooth slice organ cultures are an established *ex vivo* model to gain knowledge on the toxicity mechanisms of biomaterials on the dental mesenchymal tissues.[26,27,50,51] Compared with the *in vitro* cell cultures, the *ex vivo* tooth slice organ culture model allows the maintenance of tissue integrity and cell-cell interactions, which may provide better simulation of the clinical situation and *in vivo* microenvironment of dental mesenchymal tissues upon irritation with biomaterials.[26,27,50,51] To the best of our knowledge, this study is the first to apply resin monomer and investigate its toxicity mechanism using *ex vivo* tooth slice organ culture model. Our results revealed that TEGDMA-irritated *ex vivo* cultured tooth slice organs exhibited significantly decreased tissue viability and markedly increased autophagy as well as apoptosis. Moreover, TEGDMA-induced autophagy of *ex vivo* cultured tooth slice organs correlated with the AMPK activation and suppression of mTOR activity. We further demonstrated that NAC could protect against TEGDMA-triggered toxicity of dental mesenchymal tissues in *ex vivo* cultured tooth slice organs by inhibiting autophagy. These findings are important for understanding the clinical response of human dental mesenchymal tissues to resin monomers after operative restoration, and also provide clues for improvement of dental restorative biomaterials.

5 Conclusions

Collectively, our results showed that resin monomer TEGDMA could simultaneously activate autophagy and induce apoptosis in DMCs by triggering AMPK/mTOR signaling pathway, which could serve as a novel therapeutic target by NAC (Fig. 12). The inhibition of autophagy significantly prevented apoptosis induced by TEGDMA in DMCs, thereby suggesting the tight interplay between autophagy and apoptosis in executing TEGDMA-triggered cell death. The tooth slice organ culture

model provided further evidence of the autophagy involvement in TEGDMA-triggered dental mesenchymal tissue toxicity and as the therapeutic target by NAC *ex vivo*. Accordingly, our findings provide novel insights into the mechanisms of resin monomer-mediated cytoxicity and dental tissue damage, and highlight autophagy as the promising therapeutic target by NAC for improving dental restorative biomaterials that enables dental tissue protection.

References

1. S. Krifka, G. Spagnuolo, G. Schmalz and H. Schweikl. Biomaterials, 2013, **34**, 4555-4563.

2. M.G. Kerstin, N.D. Rena and D.H. Jeffrey. J. Mater. Chem., 2010, **20**, 8730-8746.

3. S. Krifka, C. Petzel, C. Bolay, K.A. Hiller, G. Spagnuolo, G. Schmalz and H. Schweikl. Biomaterials, 2011, **32**, 1787-1795.

4. S. Krifka, K.A. Hiller, C. Bolay, C. Petzel, G. Spagnuolo, F.X. Reichl, G. Schmalz and H. Schweikl. Biomaterials, 2012, **33**, 740-750.

5. S. Krifka, C. Petzel, K.A. Hiller, E.M. Frank, C. Bosl, G. Spagnuolo, F.X. Reichl, G. Schmalz and H. Schweikl. Biomaterials, 2010, **31**, 2964-2975.

6. F.M. Huang, Y.H. Kuan, S.S. Lee and Y.C. Chang. Environ. Toxicol., 2015, **30**, 581-588.

7. A. Bakopoulou, G. Leyhausen, J. Volk, A. Tsiftsoglou, P. Garefis, P. Koidis and W. Geurtsen. Dent. Mater., 2011, **27**, 608-617.

8. A. Eckhardt, T. Harorli, J. Limtanyakul, K.A. Hiller, C. Bosl, C. Bolay, F.X. Reichl, G. Schmalz and H. Schweikl. Biomaterials, 2009, **30**, 1665-1674.

9. K.M. Galler, H. Schweikl, K.A. Hiller, A.C. Cavender, C. Bolay, R.N. D'Souza and G. Schmalz. J. Dent. Res., 2011, **90**, 257-262.

10. H.H. Chang, M.C. Chang, H.H. Wang, G.F. Huang, Y.L. Lee, Y.L. Wang, C.P. Chan, S.Y. Yeung,

S.K. Tseng and J.H. Jeng. Acta. Biomater., 2014, **10**, 722-731.

11. M.C. Chang, L.I. Chen, C.P. Chan, J.J. Lee, T.M. Wang, T.T. Yang, P.S. Lin, H.J. Lin, H.H. Chang and J.H. Jeng. Biomaterials, 2010, **31**, 8164-8171.

12. H. Schweikl, C. Petzel, C. Bolay, K.A. Hiller, W. Buchalla and S. Krifka. Biomaterials, 2014, **35**, 2890-2904.

13. C.A. Martins, G. Leyhausen, W. Geurtsen and J. Volk. Dent. Mater., 2012, **28**, 442-448.

14. A. Eckhardt, N. Gerstmayr, K.A. Hiller, C. Bolay, C. Waha, G. Spagnuolo, C. Camargo, G. Schmalz and H. Schweikl. Biomaterials, 2009, **30**, 2006-2014.

15. H. Minamikawa, M. Yamada, F. Iwasa, T. Ueno, Y. Deyama, K. Suzuki, Y. Yawaka and T. Ogawa. Biomaterials, 2010, **31**, 7213-7225.

16. A.M. Choi, S.W. Ryter and B. Levine. N. Engl. J. Med., 2013, **368**, 651-662.

17. A.N. Hale, D.J. Ledbetter, T.R. Gawriluk and E.B. 3rd Rucker. Autophagy, 2013, **9**, 951-972.

18. P. Boya, F. Reggiori and P. Codogno. Nat. Cell. Biol., 2013, **15**, 713-720.

19. G. Das, B.V. Shravage and E.H. Baehrecke. Cold Spring Harb. Perspect. Biol., 2012, **4**, pii: a008813.

20. E. Wirawan, T. Vanden Berghe, S. Lippens, P. Agostinis and P. Vandenabeele. Cell Res., 2012, **22**, 43-61.

21. L. Zhu, J. Yang, J. Zhang and B. Peng. J. Endod., 2014, **40**, 1118-1123.

22. L. Zhu, J. Yang, J. Zhang, D. Lei, L. Xiao, X. Cheng, Y. Lin and B. Peng. Acta. Biomater., 2014, 10, 5156-5168.

23. J. Zhang, L.X. Zhu, X. Cheng, Y. Lin, P. Yan and B. Peng. J. Dent. Res., 2015, Available from URL: http://www.ncbi.nlm.nih.gov/pubmed/25724555 (DOI: 10.1177/0022034515572020).

24. M.I. Khan, A. Mohammad, G. Patil, S.A. Naqvi, L.K. Chauhan and I. Ahmad. Biomaterials, 2012, **33**, 1477-1488.

25. J. Intemann, N.E. Saidu, L. Schwind and M. Montenarh. Cell Signal., 2014, **26**, 1567-1575.

26. T.Y. Saw, T. Cao, A.U. Yap and M.M. Lee Ng. Toxicol. In Vitro, 2005, **19**, 145-54.

27. K. Trimmel, B. Cvikl, H.D. Müller, S. Nürnberger, R. Gruber, A. Moritz and H. Agis. Int. Endod. J., 2015, **48**, 252-260.

28. C.B. McLeland, J. Rodriguez and S.T. Stern. Methods Mol. Biol., 2011, **697**, 199-206.

29. C.W. Lin, M.S. Jan and J.H. Kuo. Mol. Pharm., 2014, **11**, 3002-3008.

30. E.A. Dunlop and A.R. Tee. Semin. Cell Dev. Biol., 2014, **36**, 121-129.

31. L. Yu, C.K. McPhee, L. Zheng, G.A. Mardones, Y. Rong, J. Peng, N. Mi, Y. Zhao, Z. Liu, F. Wan, D.W. Hailey, V. Oorschot, J. Klumperman, E.H. Baehrecke and M.J. Lenardo. Nature, 2010, **465**, 942-946.

32. S. Alers, A.S. Loffler, S. Wesselborg and B. Stork. Mol. Cell Biol., 2012, **32**, 2-11.

33. D.N. Tripathi, R. Chowdhury, L.J. Trudel, A.R. Tee, R.S. Slack, C.L. Walker and G.N. Wogan. Proc. Natl. Acad. Sci. U. S. A., 2013, **110**, E2950-2957.

34. A.L. Becker, N.I. Orlotti, M. Folini, F. Cavalieri, A.N. Zelikin, A.P. Johnston, N. Zaffaroni and F. Caruso. ACS Nano, 2011, **5**, 1335-1344.

35. G.L. Beretta, M. Folini, F. Cavalieri, Y. Yan, E. Fresch, S. Kaliappan, C. Hasenöhrl, J.J. Richardson, S. Tinelli, A. Fery, F. Caruso and N. Zaffaroni. Nanoscale, 2015, **7**, 6261-6270.

36. G. Filomeni, D. De Zio and F. Cecconi. Cell Death Differ., 2015, **22**, 377-388.

37. S, Wang, Y, Li, J, Fan, Z, Wang, X, Zeng, Y, Sun, P. Song and D. Ju. Biomaterials, 2014, **35**, 7588-7597.

38. Z.M. Markovic, B.Z. Ristic, K.M. Arsikin, D.G. Klisic, L.M. Harhaji-Trajkovic, B.M. Todorovic-Markovic, D.P. Kepic, T.K. Kravic-Stevovic, S.P. Jovanovic, M.M. Milenkovic, D.D. Milivojevic, V.Z. Bumbasirevic, M.D. Dramicanin and V.S. Trajkovic. Biomaterials, 2013, **33**, 7084-7092.

39. X. Ma, Y. Wu, S. Jin, Y. Tian, X. Zhang, Y. Zhao, L. Yu and X.J. Liang. ACS Nano, 2011, **5**, 8629-8639.

40. Y. Cao and D.J. Klionsky. Cell Res., 2007, **17**, 839-849.

41. G. Marino, M. Niso-Santano, E.H. Baehrecke and G. Kroemer. Nat. Rev. Mol. Cell Biol., 2014, **15**, 81-94.

42. S. Mukhopadhyay, P.K. Panda, N. Sinha, D.N. Das and S.K. Bhutia. Apoptosis, 2014, **19**, 555-566.

43. A.D. Rubinstein and A. Kimchi. J. Cell Sci., 2012, **125**, 5259-5268.

44. L.A. Booth, S. Tavallai, H.A. Hamed, N. Cruickshanks and P. Dent. Cell Signal., 2014, **26**, 549-555.

45. Y. Wu, X. Wang, H. Guo, B. Zhang, X.B. Zhang, Z.J. Shi and L. Yu. Autophagy, 2013, **9**, 595-603.

46. X. Wen, J. Wu, F. Wang, B. Liu, C. Huang and Y. Wei. Free Radic. Biol. Med., 2013, **65**, 402-410.

47. B.B. Zhang, D.G. Wang, F.F. Guo and C. Xuan. Fam. Cancer, 2015, **14**, 19-23.

48. D.H. Lee, B.S. Lim, Y.K. Lee, S.J. Ahn and H.C. Yang. Dent. Mater., 2006, **22**, 1086-1092.

49. Y. Samuni, S. Goldstein, O.M. Dean and M. Berk. Biochim. Biophys. Acta., 2013, **1830**, 4117-4129.

50. P.E. Murray, P.J. Lumley, H.F. Ross and A.J. Smith. Biomaterials, 2000, **21**, 1711-1721.

51. S.A. Alfaqeeh and A.S. Tucker. J. Vis. Exp., 2013, **81**, e50824.

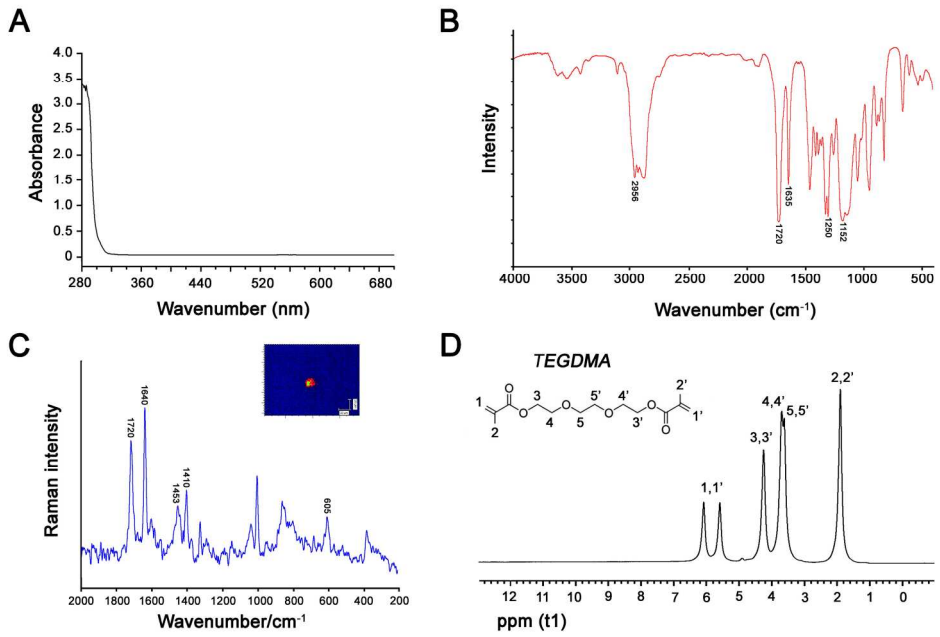

Fig. 1 Physical and chemical characterization of resin monomer TEGDMA. UV-VIS (A), ATR-FTIR (B), micro-Raman (C), and 1H NMR analysis of TEGDMA.
108x73mm (600 x 600 DPI)

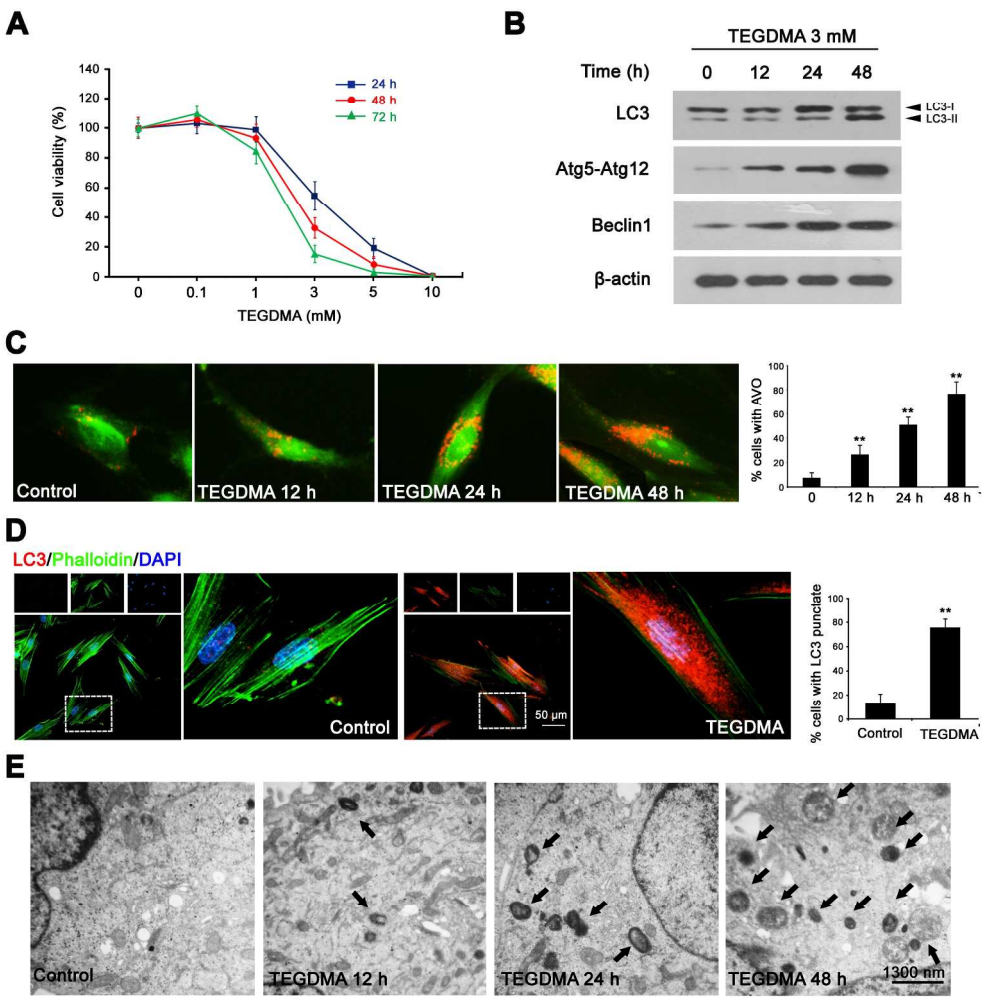

Fig. 2 TEGDMA activated autophagy in DMCs. (A) Cell viability of DMCs exposed to various concentrations of TEGDMA as measured by CCK-8 assay. (B) Expression levels of LC3, Atg5-Atg12 complex, Beclin 1, and β-actin as shown by Western blot analysis. (C) Detection and quantification of TEGDMA-induced formation of yellow-orange AVOs. **P<0.01 vs. the control group. (D) Detection and quantification for TEGDMA-induced punctate pattern of LC3 immunostaining colocalized with stress fibers. **P<0.01 vs. the control group. Results are expressed as the mean ± SD of three independent experiments. (E) Observation of TEGDMA-induced autophagosomes (arrow heads) via TEM.
159x159mm (600 x 600 DPI)

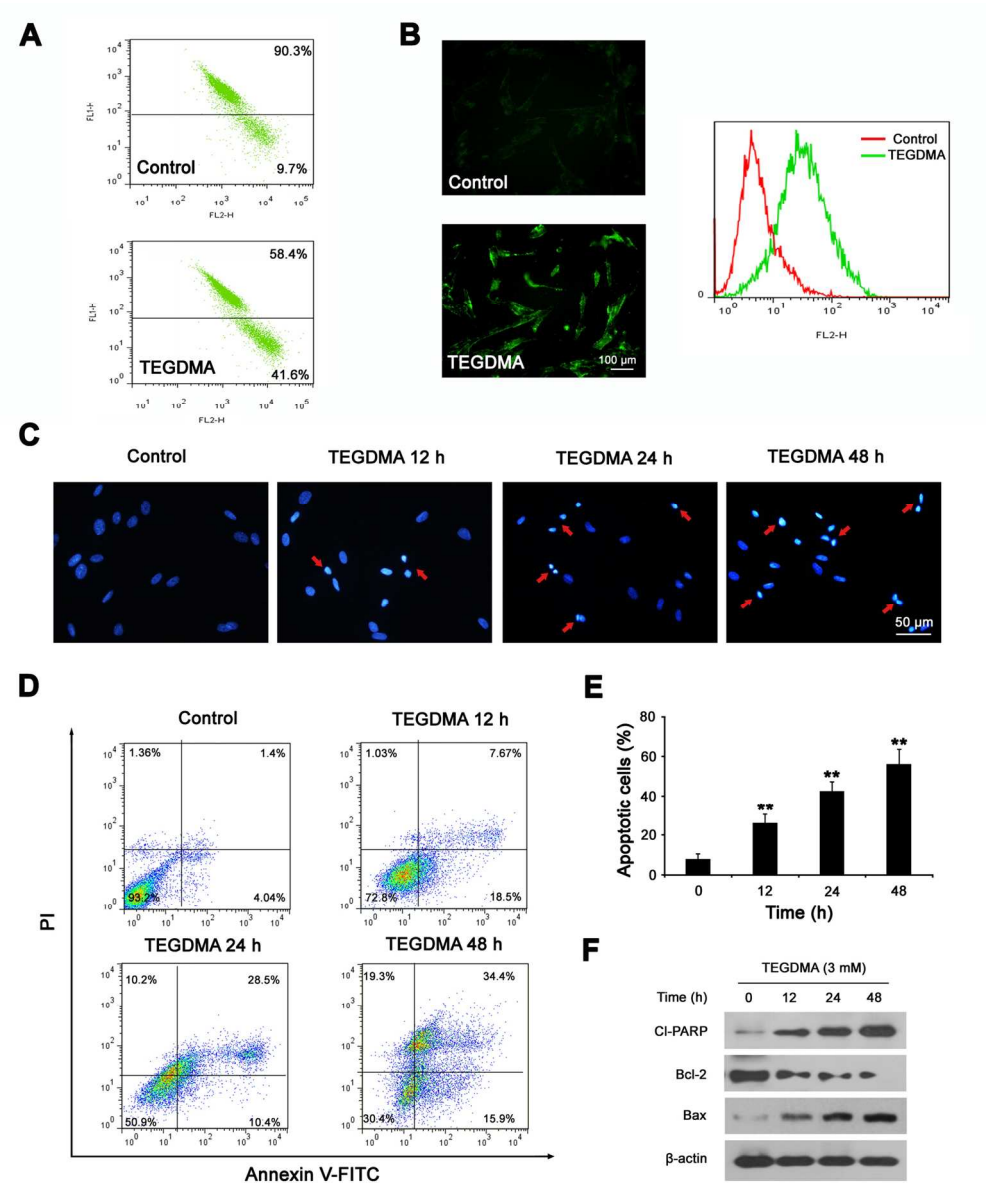

Fig. 3 TEGDMA induced ROS generation and apoptosis in DMCs. (A) Mitochondrial membrane potential of DMCs exposed to TEGDMA, as determined by using JC-1 via flow cytometry. (B) ROS generation of DMCs exposed to 3 mM TEGDMA detected with DCF-DA by fluorescence microscopy and flow cytometry. (C) Morphological changes captured with fluorescence microscopy via Hoechst 33258 staining. (D) Cell apoptosis of DMCs exposed to various concentrations of TEGDMA presented as 2D density plots measured via flow cytometry after Annexin V-PI staining. (E) Quantification for TEGDMA-induced apoptosis via flow cytometry after Annexin V-PI staining. **P<0.01 vs. the control group. Results are expressed as the mean ± SD of three independent experiments. (F) Western blot analysis was performed to determine the protein expression levels of cleaved PARP (Cl-PARP), Bcl-2, Bax, Bad, and β-actin.
160x194mm (300 x 300 DPI)

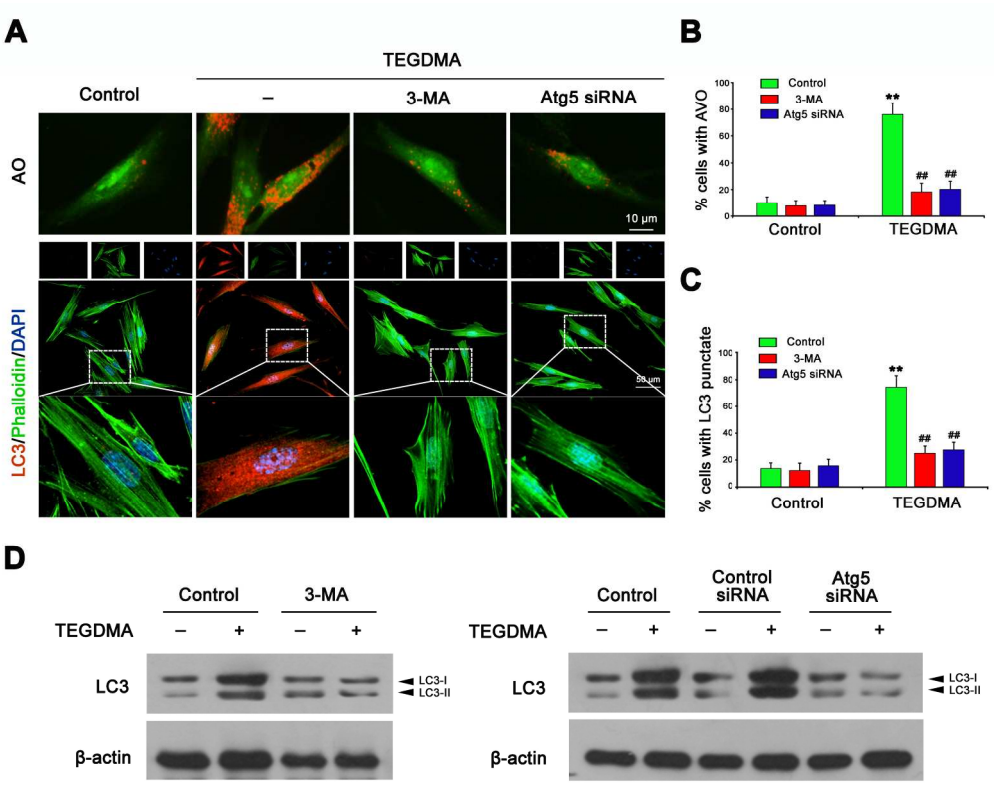

Fig. 4 Inactivation of Atg5 prevented TEGDMA-induced autophagy in DMCs. DMCs were pretreated with 3-MA or transfected with Atg5-siRNA, and then exposed to TEGDMA for 48 h. (A) Detection of TEGDMA-induced AVOs formation by acridine orange (AO) staining and punctate pattern of LC3 immunostaining colocalized with stress fibers. (B) Quantification for TEGDMA-induced AVOs formation and (C) punctuate pattern of LC3 immunostaining. **P<0.01 vs. the control group, ##P<0.01 vs. the TEGDMA group. Results are expressed as the mean ± SD of three independent experiments. (D) Protein expression level of LC3 and β-actin in TEGDMA-treated DMCs after pretreatment with 3-MA or transfection with Atg5-siRNA as evaluated with Western blot analysis.
127x101mm (600 x 600 DPI)

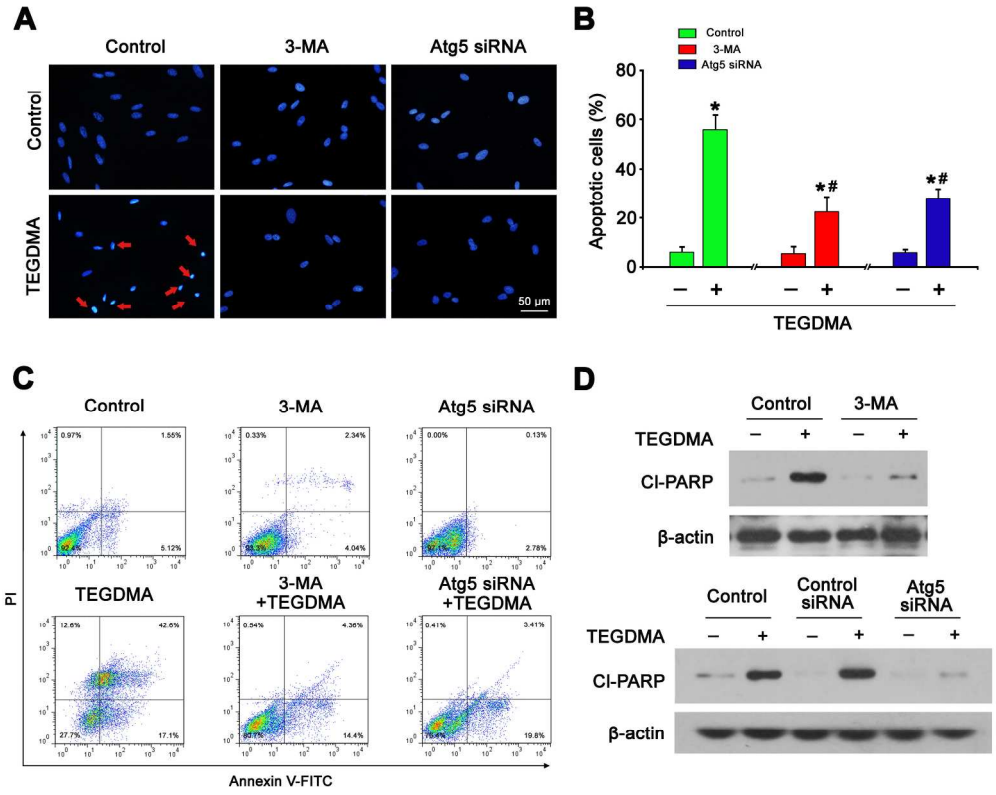

Fig. 5 Autophagy inhibition prevented TEGDMA-induced apoptosis in DMCs. DMCs were transfected with Atg5-siRNA or pretreated with 3-MA and then exposed to TEGDMA for 48 h. (A) Morphologic changes captured by fluorescence microscopy and Hoechst 33258 staining. (B) Quantification for TEGDMA-induced apoptosis via Annexin V-PI staining and flow cytometry after pretreatment with 3-MA or transfection with Atg5-siRNA. *P<0.05 vs. the control group, #P<0.05 vs. the TEGDMA group. Results are expressed as the mean ± SD of three independent experiments. (C) Cell apoptosis of DMCs pretreated with 3-MA or Atg5-siRNA followed by TEGDMA exposure determined via flow cytometry after Annexin V-PI staining and presented as 2D density plots and. (D) Protein expression level of cleaved PARP (Cl-PARP) and β-actin in TEGDMA-treated DMCs after transfection with Atg5-siRNA or pretreatment with 3-MA as evaluated with Western blot analysis.
135x115mm (600 x 600 DPI)

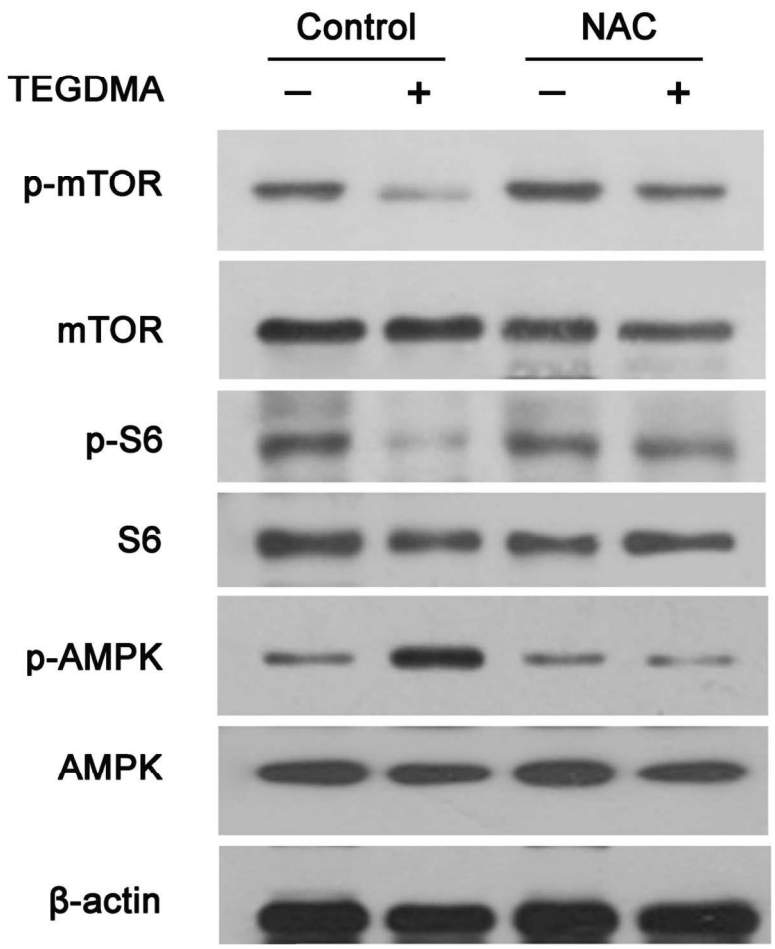

Fig. 6 TEGDMA initiated activation AMPK/mTOR signaling in DMCs, which could be targeted by NAC. DMCs were pretreated with NAC and exposed to 3 mM TEGDMA. The expression levels of p-mTOR, mTOR, p-S6, S6, p-AMPK, AMPK, and β-actin were detected by Western blot analysis.
79x78mm (600 x 600 DPI)

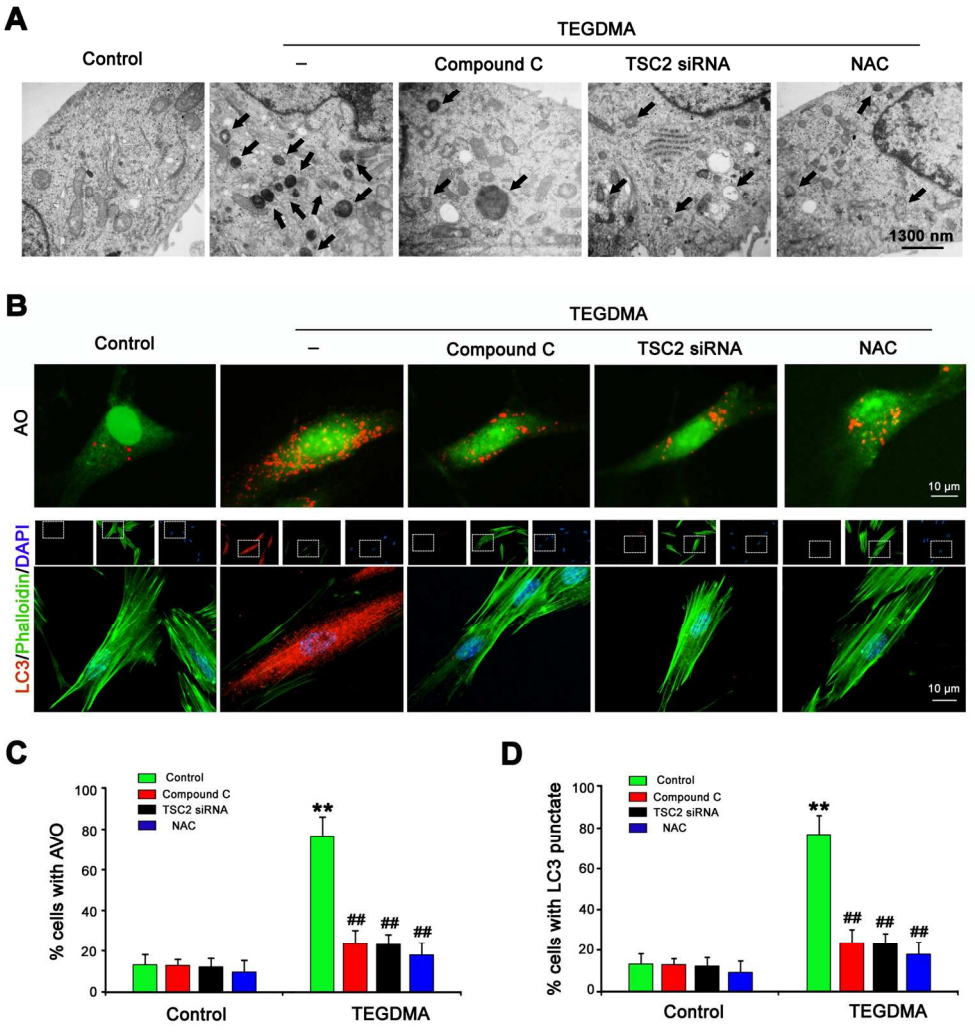

Fig. 7 AMPK/mTOR signaling was involved in TEGDMA-induced autophagy, which could be abrogated by NAC. (A) Detection of TEGDMA-induced autophagosomes (black arrowheads) via TEM after transfection with TSC2-siRNA or pretreatment with Compound C or NAC. (B) Detection of TEGDMA-induced AVOs formation by acridine orange (AO) staining and punctate pattern of LC3 immunostaining colocalized with stress fibers after transfection with TSC2-siRNA or pretreatment with Compound C or NAC. Quantification for TEGDMA-induced AVOs formation (C) and punctate pattern of LC3 immunostaining (D). **P<0.01 vs. the control group, ##P<0.01 vs. the TEGDMA group. Results are expressed as the mean ± SD of three independent experiments.
170x181mm (300 x 300 DPI)

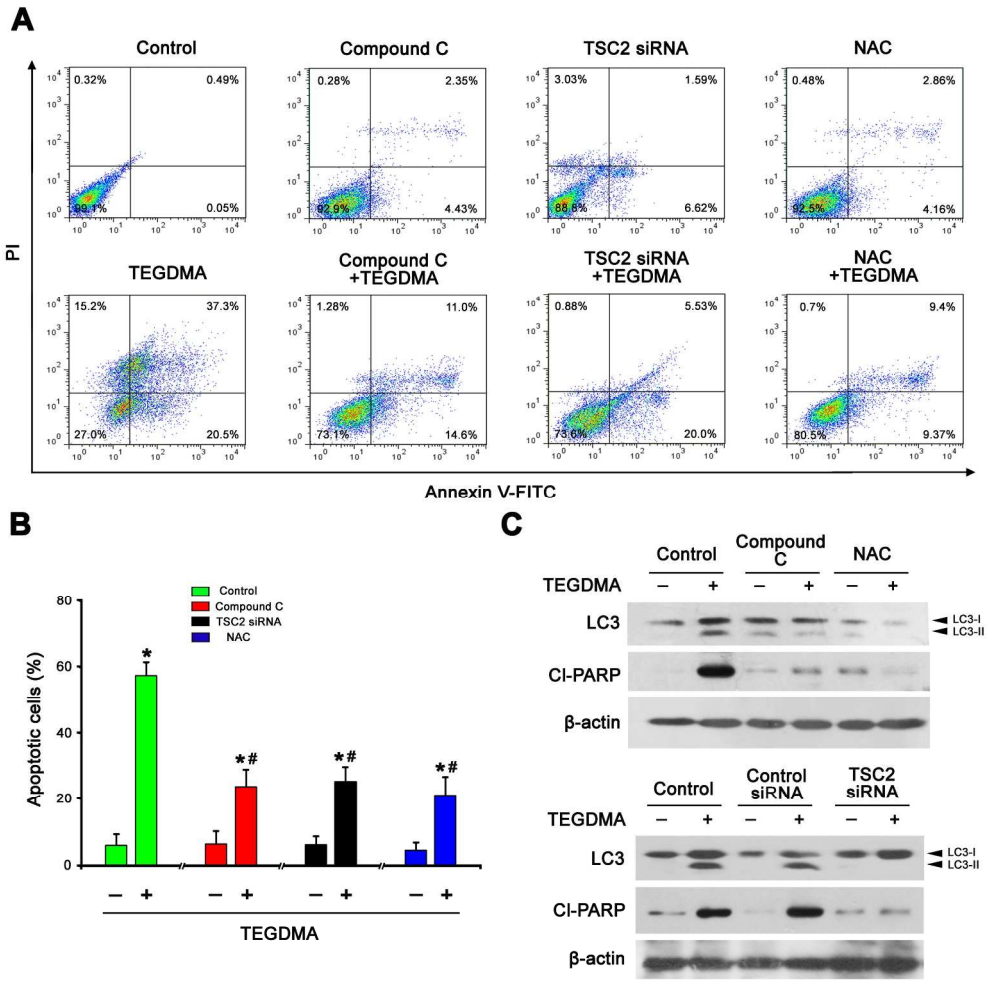

Fig. 8 AMPK/mTOR-dependent autophagy as the therapeutic target of NAC against TEGDMA-induced toxicity in DMCs. (A) Cell apoptosis of DMCs pretreated with Compound C, TSC2-siRNA transfection, or NAC, and exposed to TEGDMA is presented as 2D density plots and measured by flow cytometry after Annexin V-PI staining. (B) Quantification for TEGDMA-induced apoptosis via Annexin V-PI staining and flow cytometry after pretreatment with Compound C, TSC2-siRNA transfection, or NAC. *P<0.05 vs. the control group, #P<0.05 vs. the TEGDMA group. Results are expressed as the mean ± SD of three independent experiments. (C) Protein expression level of LC3, cleaved PARP (Cl-PARP), and β-actin in TEGDMA-treated DMCs after pretreatment with Compound C, TSC2-siRNA transfection, or NAC, as evaluated with Western blot analysis.
159x159mm (600 x 600 DPI)

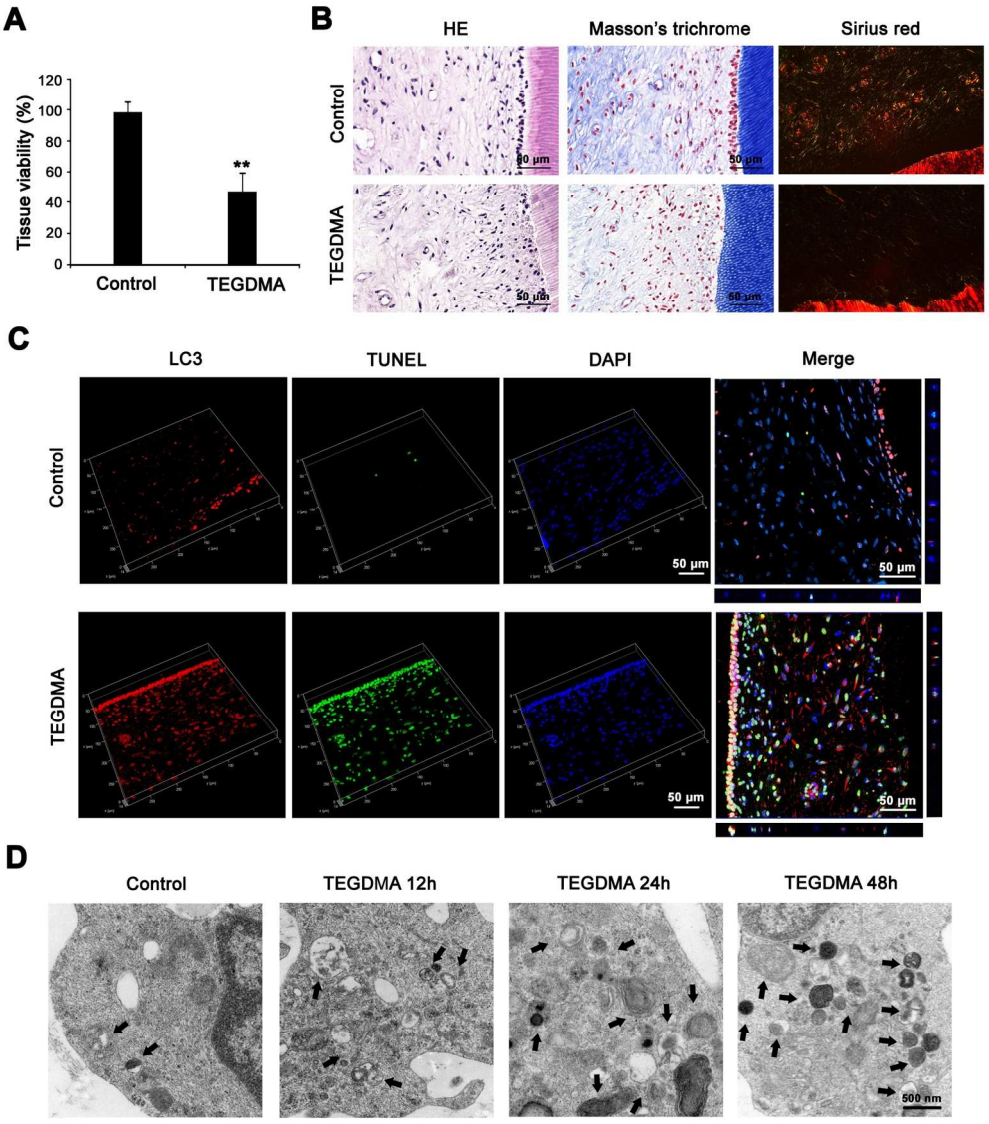

Fig. 9 TEGDMA activated autophagy of dental mesenchymal tissues in a tooth slice organ culture model ex vivo. (A) Tissue viability of tooth slice organ culture exposed to TEGDMA as measured by CCK-8 assay. **P<0.01 vs. the control group. Results are expressed as the mean ± SD of three independent experiments. (B) HE, Masson trichrome, and Sirius red staining were conducted to evaluate the changes of cell morphology and extracellular matrix of pulp-dentin complex. (C) Double immunofluorescent staining of LC3 (red) colocalized with TUNEL signal (green) in the ex vivo cultured tooth slice organs treated with TEGDMA followed by imaging by confocal microscopy. (D) Detection of TEGDMA-induced autophagosomes (black arrowheads) in the ex vivo cultured tooth slice organs via TEM.
183x211mm (300 x 300 DPI)

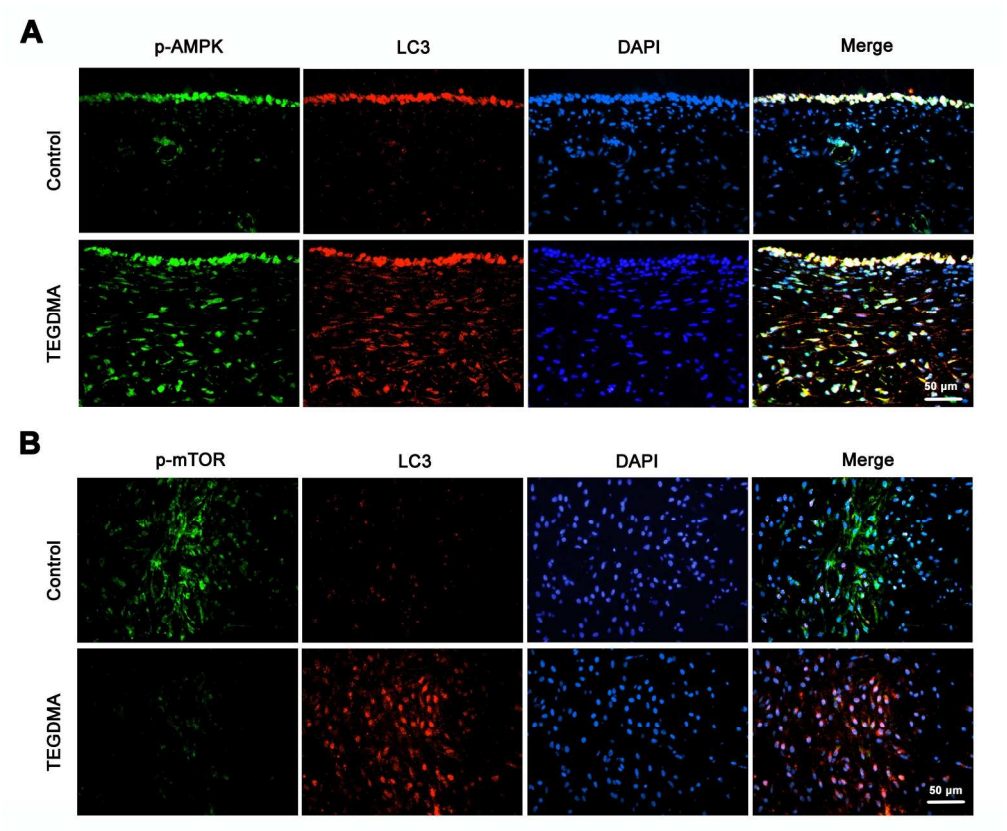

Fig. 10 TEGDMA-triggered autophagy of ex vivo cultured human tooth slice organs correlated with the AMPK activation and suppression of mTOR activity. Double immunofluorescent staining of p-AMPK (A) or p-mTOR (B) colocalized with LC3 in the ex vivo cultured dental mesenchymal tissues treated with TEGDMA.
132x109mm (600 x 600 DPI)

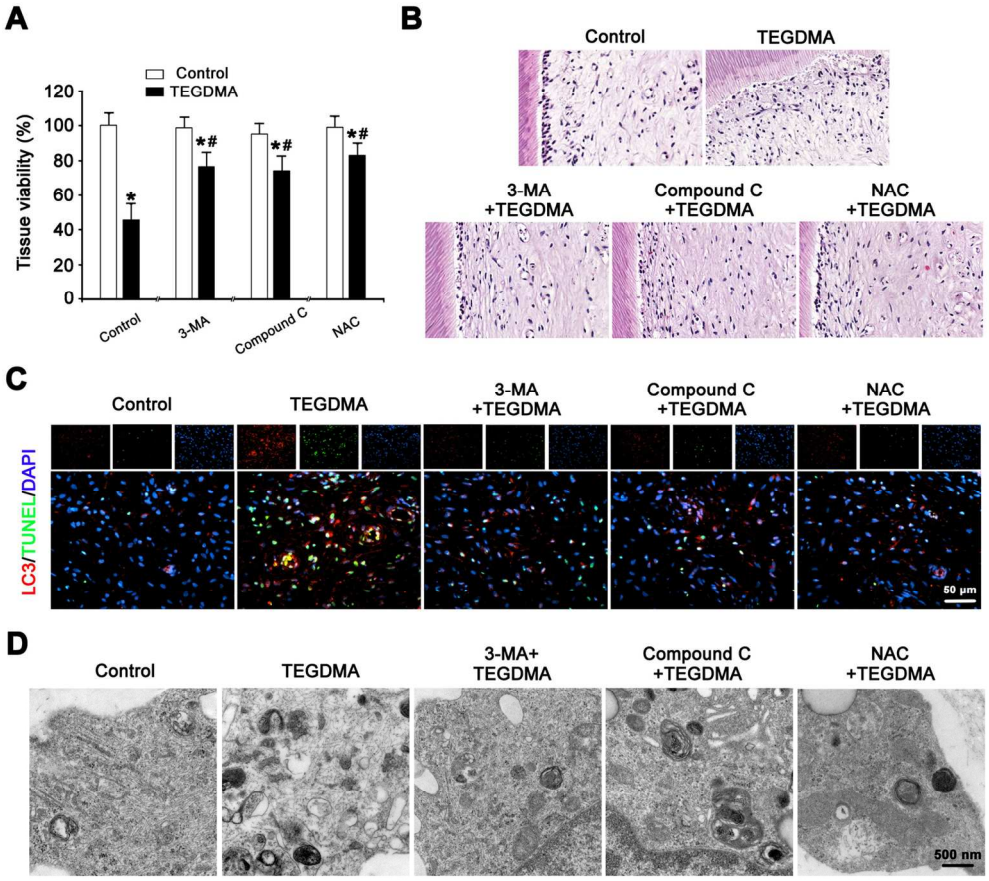

Fig. 11 AMPK/mTOR-related autophagy as the therapeutic target of NAC against TEGDMA-induced dental mesenchymal tissue toxicity in ex vivo cultured human tooth slice organs. (A) Tissue viability of ex vivo cultured tooth slice organs exposed to TEGDMA after pretreatment with 3-MA, Compound C, or NAC, as measured by CCK-8 assay. *P<0.05 vs. the control group, #P<0.05 vs. the TEGDMA group. Results are expressed as the mean ± SD of three independent experiments. (B) The HE morphology of pulp-dentin complex of ex vivo cultured tooth slice organs exposed to TEGDMA after pretreatment with 3-MA, Compound C, or NAC. (C) Double immunofluorescent staining of LC3 (red) colocalized with TUNEL signal (green) in the ex vivo cultured tooth slice organs exposed to TEGDMA after pretreatment with 3-MA, Compound C, or NAC. (D) Detection of TEGDMA-induced autophagosomes in the ex vivo cultured tooth slice organs via TEM after pretreatment with 3-MA, Compound C, or NAC.
143x129mm (300 x 300 DPI)

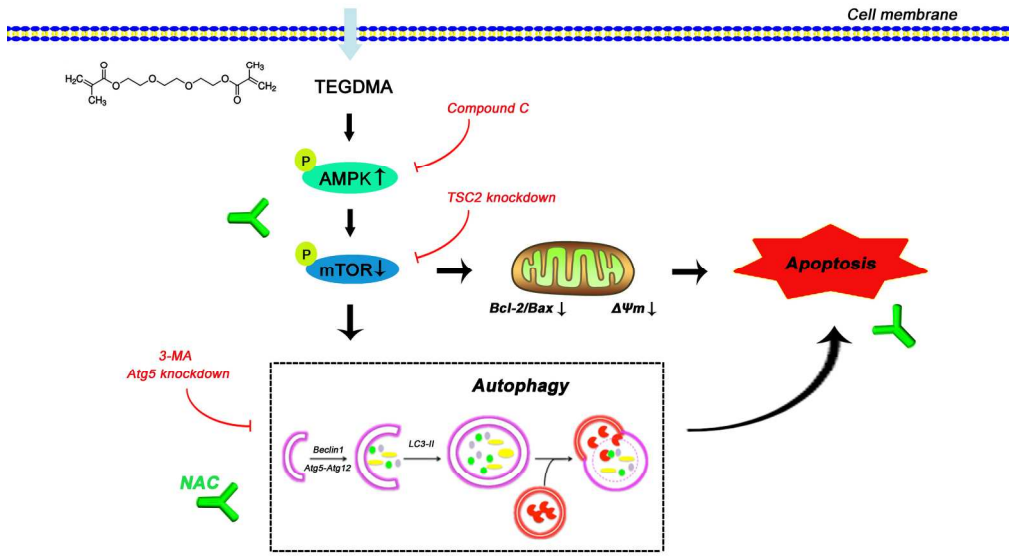

Fig. 12 Proposed schematic model of autophagy involvement in resin monomer-initiated toxicity of DMCs and as the novel therapeutic target by NAC. TEGDMA with the methacrylic structure, could prompt the activation of AMPK/mTOR signaling and induce autophagy of DMCs in vitro and human tooth slice organs ex vivo. Moreover, the TEGDMA-activated autophagy occurs via AMPK/mTOR pathway and is pro-apoptotic, which could be prevented by the anti-oxidative amino acid derivative NAC.
98x60mm (600 x 600 DPI)

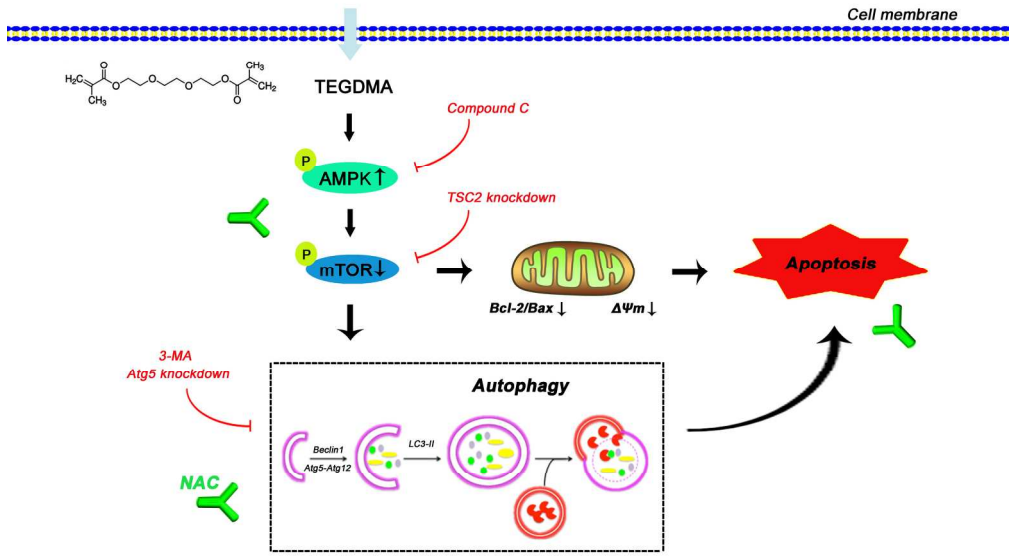

Graphic abstract: Proposed schematic model of autophagy involvement in resin monomer-initiated toxicity of dental mesenchymal cells and as the novel therapeutic target by NAC.
98x60mm (600 x 600 DPI)